JOURNAL OF AGRICULTURAL AND FOOD CHEMISTRY

Agricultural and Environmental Chemistry

Antifungal Application of Rosin Derivatives from Renewable Pine Resin in Crop Protection

Pan Tao, Chengyu Wu, Jin Hao, Yanqing Gao, Xiaohua He, Jian Li, Shibin Shang, Zhanqian Song, and Jie Song

J. Agric. Food Chem., **Just Accepted Manuscript** • DOI: 10.1021/acs.jafc.0c00562 • Publication Date (Web): 19 Mar 2020

Antifungal Application of Rosin Derivatives from Renewable Pine Resin in Crop Protection

Pan Tao,[†] Chengyu Wu,[†] Jin Hao,[‡] Yanqing Gao,[‡] Xiaohua He,[‡] Jian Li,[*,†] Shibin Shang,[§] Zhanqian Song,[§] and Jie Song[*,∥]

[†]College of Forestry, Northwest A&F University, Yangling, Shaanxi 712100, People's Republic of China

[‡]College of Plant Protection, Northwest A&F University, Yangling, Shaanxi 712100, People's Republic of China

[§]Institute of Chemical Industry of Forest Products, Chinese Academy of Forestry, Nanjing, Jiangsu 210042, People's Republic of China

[∥]Department of Chemistry and Biochemistry, University of Michigan-Flint, Flint, MI 48502, United States

Corresponding Authors:

*E-mail: ericlee99@nwsuaf.edu.cn. Telephone: +86-29-87082392 (Jian Li).

*E-mail: jiesong@umich.edu. Telephone: (810) 762-3275 (Jie Song).

ABSTRACT： In the current work, we synthesized two series of dehydroabietyl amide derivatives from natural product rosin and evaluated their antifungal effects on *Valsa mali, Phytophthora capsici, Botrytis cinerea, Sclerotinia sclerotiorum* and *Fusarium oxysporum*. *In vitro* and *in vivo* antifungal activities results indicated that rosin-based amide compounds containing thiophene heterocycles had better inhibitory effects on *B. cinerea*. In particular, compound **5b** (5-fluoro-2-thiophene dehydroabietyl amide) exhibited the excellent antifungal properties against *B. cinerea* with EC_{50} of 0.490 mg/L, which was lower compared to the positive control penthiopyrad (0.562 mg/L). Physiological and biochemical studies showed that the primary action mechanism of compound **5b** on *B. cinerea* changes mycelial morphology, increases cell membrane permeability and inhibits TCA pathway in respiratory metabolism. Furthermore, QSAR and SAR studies revealed that charge distribution of rosin-based amides derivatives have a key role in the antifungal activity through the hydrogen bonding, conjugation and electrostatic interaction between the compounds and the receptors of target. To sum up, this study contributes to the development of rosin-based antifungal agents with novel structure and preferable biological activity.

KEYWORDS: *rosin*, *amide*, *thiophene heterocycle*, *antifungal activity*, *action mechanism*, *QSAR*

INTRODUCTION

Pesticides have an important role in the agricultural production, especially in reducing labor intensity, avoiding pests and diseases, cultivating new crop varieties, and similar [1]. Moreover, their use brings enormous economic and social benefits for human development [2]. Fungicides, which are among the most important types of pesticides, can control plant diseases caused by various pathogenic microorganisms by killing or inhibiting the growth of pathogens [3]. In fact, the usage of fungicides has become one of the most economical and effective ways to reduce the huge losses in agriculture caused by plant diseases [4].

Over recent years, the new fungicides have become the research hot spot, resulting in development of fungicides with novel mechanisms [5]. Among them, succinate dehydrogenase inhibitors (SDHIs) are the most innovative ones because of their high efficiency, broad spectrum and novel mechanism [6]. As important amide fungicides, SDHIs can inhibit the growth of pathogens, eventually killing them through their respiratory chain electron transport systems [7]. Nevertheless, the widespread use of fungicides has produced more and more resistance problems [8, 9]. Meanwhile, their residual toxicity and negative impact on the environment still haven't been resolved effectively [10]. The research and development of new fungicides with natural products as the lead compounds may be an effective way to overcome these problems [11].

There are many kinds of natural products, and they have various biological activities, unique action mechanism, easy degradation and good environmental compatibility, which are important alternatives for development of green fungicides

[12]. At present, natural products not only provide a large number of novel lead compounds for the development of fungicides, but also probes that can lead to discovery of new targets [13]. Especially, the active ingredients derived from plants (secondary metabolism, are synthesized in the process of plant co-evolution to resist the invasion of outer pathogens) have become the significant part of developing green bio pesticides [14].

Rosin is a kind of natural resin that is secreted from pine trees. Rosin and its derivatives have important research and development values as pesticides, herbicides and bacteriostats in the field of agrochemicals. However, few studies have investigated its application in antifungal activities [15]. Specially, the specific action mode and regulation response mechanism of ternary phenanthrene ring structure and chiral centers of rosin and/or its derivatives on fungi target site have not received adequate attention [16, 17].

Based on our previous research results, in the present study we designed and synthesized series of rosin-based amide antifungal agents. Inspired by penthiopyrad (one of the typical SDHIs), and with the aim to further improve their antifungal effects, thiophene heterocycles were introduced into one of series of rosin-based amide derivatives. In order to explore the preliminary mechanisms of action of rosin-based amide derivatives, the morphological changes of mycelia cell wall and the antifungal effects on the permeability of mycelia cell membrane and respiratory metabolism of fungi were examined. Meanwhile, the relationship between the molecular physicochemical characteristics of rosin-based amide compounds and

antifungal activity were investigated by SAR and QSAR analysis. The obtained results provide a new insight for the development of sustainable pine-based fungicide in crop protection.

MATERIALS AND METHODS

Materials and Structural Characterization. All chemical reagents and solvents were purchased from commercial company. The melting point was determined by Hannon MP-450 melting point apparatus (Hanon Subsidiary Company, Jinan, China). Infrared spectroscopy (IR) analyses of the dehydroabietyl amide derivatives were measured on a Nicolet IS10 infrared spectrophotometer (Thermo Nicolet Co., Madison, USA). ^{1}H NMR spectra were recorded on a Bruker AVANCE-III (500 MHz) spectrometer and ESI mass spectra were detected on a Bruker Q-TOF mass spectrometer (Bruker Co., Karlsruhe, Germany). Elemental analyses were determined on a Vario EL-III (Elementar Co., Hanau, Germany). Potato dextrose agar (PDA) culture medium was prepared with potatoes, agar, glucose and distilled water. The preparation method of potato glucose broth (PDB) culture medium is similar to that of PDA, except agar was added.

Synthesis of Dehydroabietyl Amide Compounds (3a-p). Dehydroabietic acid (**1**, **DHAA**) and dehydroabietyl chloride (**2**) were prepared according to previously reported methods [15]. Dehydroabietic amide compounds (**3a-p**) were obtained by compound **2** and aromatic amines or ammonium hydroxide by nucleophilic reaction. In short, 10 mmol amine, 40 mL dichloromethane (DCM) and 2 mL triethylamine (Et_3N) were added to 250 mL flask and evenly stirred. Compound **2** (3.19 g; 10

mmol) was added to the above solution and completed in 30 minutes. After 12 h of reaction, the mixture solution was washed to neutral in turn with acid and water. Finally, the crude product was obtained by drying with anhydrous magnesium sulfate and removing the solvent under vacuum. The title compounds (**3a-o**) were purified by recrystallization with ethanol. Compound **3p** was prepared with the similar method as above-mentioned, except that in compound **2** the 10 mL ammonia water (80%) was added to 40 mL tetrahydrofuran (THF) at low temperature (0 °C). The synthetic routes of compounds **3a-p** are shown in **Scheme 1**.

Synthesis of Dehydroabietyl Amides Containing the Thiophene Heterocyclic Group. The preparation of series of compounds (**5a-n**) was similar to that of **3a-p**. Briefly, 2-thenoylchloride and 5-substituted analogs were prepared by reaction of thionyl chloride (1.79 g, 15 mmol) on the corresponding thiophene-2 carboxylic acids (10 mmol) in DCM under reflux. Then, above acyl chloride was added to compound **4** (prepared by reduction of **3n** with lithium aluminium hydride) with the same molar amount at room temperature. After 12 h reaction, the target compounds **5a-n** were obtained by acid washing, water washing and recrystallization with ethanol. The synthetic routes of the compounds (**5a-n**) are shown in **Scheme 2**.

***In Vitro* Antifungal Activity.** According to the literature, the growth rate method was used to determine the *in vitro* antifungal activity of synthesized compounds [18]. A total of 50 mg of tested compounds (including positive control, penthiopyrad) were added to 5 mL DMSO to prepare initial solution with a concentration of 10 mg/mL. Then, the above solution was diluted to 500.00, 200.00, 100.00, 50.00, 25.00, 12.50,

6.25, 3.13, 1.56, and 0.78 mg/L by PDA medium. Equal amount of DMSO without tested compounds was used as negative control. Activated pathogens were punched with a 5 mm diameter puncher, and were inoculated in the center of the medicated medium in a 25 °C incubator. Each experiment was run in triplicate and the statistical results were averaged. The antifungal activity results were expressed by the inhibition rate of mycelium growth (*IR*) in Eq. (1). Linear regression equation was established by SPSS statistics software, and correlation analysis was carried out to determine the inhibitory activity of the dehydroabietyl amide derivatives against different pathogens.

$$IR\ (\%) = (B\text{-}T)/\ B \times 100 \qquad (1)$$

where *B* and *T* are colony growth diameter of blank control and treated compounds, respectively.

***In Vivo* Antifungal Activity.** The protective efficacy of test compounds on strawberry leaves inoculated with *B. cinerea* was determined by *in vivo* tissue method [19]. The test compounds were dissolved in DMSO, distilled water and Triton-100 (0.2%) and prepared into three concentrations of 100, 50 and 25 mg/L, respectively. The negative control was DMSO solution containing 0.2% Triton-100 and the positive control was penthiopyrad. First, the strawberry leaves similar in size and growth status and without being infected by any of other pathogens were selected and washed with clean water. Then, the fresh strawberry leaves were evenly sprayed with test solution and naturally dried. In the tray, the strawberry leaves were inoculated with *B. cinerea* and small holes on the tested leaves were pricked with inoculation

147 needles. The inoculated strawberry leaves were cultured in the incubator (25 °C and
148 80% relative humidity) for 48-72 h. The plaque diameters of *B. cinerea* on strawberry
149 leaves were measured by cross-over method. Each experiment was run in triplicate.
150 The protective efficacy (*PE*) was used to assess the antifungal effect on *B. cinerea* in
151 Eq. (2):

152 $$PE\ (\%) = (C - T)/\ (C\text{-}5) \times 100 \qquad (2)$$

153 where *C* and *T* are colony expansion sums of control and treated strawberry leaves,
154 respectively.

155 **Effect of dehydroabietyl amide (5b) on mycelial morphology of *B. cinerea.*** *B.*
156 *cinerea* was cultured in a 90 mm culture dish. When the mycelia grew to 70 mm in
157 diameter, fresh fungus dishes (5 mm in diameter) were made from the edge of the
158 colonies. The mycelia were inoculated on PDA medium plates containing no
159 compound (negative control) and amide **5b** with a concentration of 20 mg/L,
160 respectively. Then, the mycelia were cultured at 25 °C for 2 days. The mycelia cell
161 wall structure of *B. cinerea* at the top of each treated colonies were selected and
162 observed under an S-3400N scanning electron microscope (SEM) (Hitachi, Ltd.,
163 Tokyo, Japan).

164 **Effect of dehydroabietyl amide (5b) on cell membrane permeability of *B.***
165 ***cinerea.*** The tested strains were cultured on PDA plate at 25 °C for 3 days and made
166 into a 7 mm diameter disc. Then, the strains were placed in PDB culture medium and
167 cultured by shaking (25 °C, 120 rpm) for 3 days. The mycelia were filtered and
168 washed with distilled water and put into centrifugal tube, and then 10 mL of

compound **5b** (25 mg/L) and distilled water were added into the centrifugal tube, respectively. Finally, the mycelia were oscillated (120 rpm) in water bath at constant temperature of 28 °C at different times. The conductivity was measured by a CON510 Eutech/Oakton conductometer (OAKTON Instruments, Waltham, USA). The negative control was mycelia with distilled water. The conductivity of the compound **5b** was determined at 0, 30, 60, 90, 120, 180, 240, 300, 360, 420, 480, 540 min, and finally boiled (dead treatment) to determine the conductivity. The relative permeability was calculated for each measurement, and then the permeability of cell membranes was compared according to the conductivity. Each experiment was run in triplicate.

Effect of dehydroabietyl amide (5b) on the respiratory metabolism of *B. cinerea*. The respiratory oxygen consumption rate of *B. cinerea* was measured by oxygen electrode method [20]. A total of 50 mg fresh mycelia were added into 1 mL of medium solution (0.9 mL of phosphate buffer solution with concentration of 0.1 mol/L, pH = 7.2 and 0.1 mL of glucose solution with concentration of 2%). After stirring for 5 mins, dissolved oxygen was measured by a JPB-607A dissolved oxygen meter (INESA Scientific Instrument Co., Shanghai, China). Then, three typical respiratory inhibitors, namely, malonic acid, iodoacetic acid and sodium phosphate (inhibiting tricarboxylic acid cycle (TCA) pathway, Embden-Meyerhof-Parnas (EMP) pathway and hexose monophosphate pathway (HMP), respectively) and/or test agents (25 mg/L) were added. Respiration rate of mycelia (O_2, μmol/g·min) was calculated from the change of oxygen content in medium. The inhibition rate of mycelia

191 respiration (IR_r) was calculated according to the respiration rate of mycelia before and
192 after adding test agents in Eq. (3):

193 $$IR_r\ (\%) = (R_0\text{-}R_1)/\ R_0 \times 100 \qquad (3)$$

194 where R_0 and R_1 are respiration rate of mycelia before and after adding tested agents.

195 According to the respiration rate of mycelia before and after the addition of
196 typical inhibitors, the superposition rate of tested agents with typical inhibitors (R_R)
197 was calculated in Eq. (4):

198 $$R_R\ (\%) = (R_1\text{-}R_1')/\ R_1 \times 100 \qquad (4)$$

199 where R_1 is respiration rate of mycelia after adding test agents and R_1' is the
200 respiratory rate of mycelia after adding test agents and typical inhibitors.

201 **QSAR.** The density functional theory (DFT) method of Gaussian 16 (Gaussian,
202 Inc., Wallingford, USA) was used to optimize the molecular structures and calculate
203 the minimum energy of synthesized compounds [21]. Some important molecular
204 structure properties were obtained, such as molecular energy, dipole, atomic charge
205 distribution, molecular orbitals and orbital energies, electron density and electrostatic
206 potential. Then, the molecular structures and antifungal activities were linearly
207 regressed by CODESSA software 2.7.15 (Semichem, Inc., Shawnee, USA), and the
208 quantitative relationship models were constructed. Finally, the models were validated
209 and the antifungal activities were predicted by the built best model. The lowest
210 unoccupied molecular orbital (*LUMO*) of compound **5b** was viewed, plotted and
211 visualized by MO editor in GaussView 6.0. The charge distribution of compound **5b**
212 was obtained by viewing the optimized compound molecule result. The molecular

electrostatic potential (MEP) plot and contour map of compound **5b** were generated by surface and contour action in Surface/Contour of GaussView 6.0, respectively.

RESULTS AND DISCUSSION

The preparation of dehydroabietyl amide derivatives. The reactivity of carboxyl or amino groups on compound **1** (DHAA) or **4** (dehydroabietic amine) are low because of the steric hindrance of tricyclic phenanthrene skeleton of rosin [22, 23]. Therefore, the preparation of rosin-based amides requires more harsh conditions, such as high temperature, high pressure and the addition of catalysts. However, at higher temperatures, rosin is prone to decarboxylation or oxidation, resulting in darker color and more by-products [24]. Nonetheless the reactivity can be greatly improved by converting carboxylic acid into active intermediates acyl chloride. In the present study, we used thionyl chloride as the acylation reagent so as to easily obtain acyl chloride. Because the by-product is gas, the crude product can be easily purified, obtaining the yield of acyl chloride as high as 95-98%. Moreover, in the process of reaction, amides were formed and hydrochloric acid (HCl) was produced. We used triethylamine (Et_3N) as acid binding agent to react with HCl and to form corresponding salt precipitation, thus promoting the reaction with higher yield and less by-products. All reaction processes were monitored by thin layer chromatography (TLC).

***In vitro* antifungal activity against *B. cinerea* and structure-activity relationship.** The antifungal results showed that two series of rosin-based amide derivatives had certain inhibitory effect on fungi *V. mali, P. capsici, B. cinerea, S.*

235 *sclerotiorum* and *F. oxysporum*. However, most of the synthesized compounds
236 showed lower antifungal activity against *V. mali*, *P. capsici*, *S. sclerotiorum* and *F.*
237 *oxysporum*, but showed better inhibitory effect on *B. cinerea* (**Figure 1a**).

238 According to the statistical results of the structure and activity of the synthesized
239 compounds, the inhibitory effect on *B. cinerea* of the rosin-based amide derivatives
240 containing thiophene heterocyclic structure (**5a-n**) was better than that of the amide
241 derivatives (**3a-p**) without heterocyclic structure (**Table 1**). The EC_{50} value of amide
242 derivatives containing thiophene heterocyclic structure (**5a-n**) ranged from 0.490 to
243 78.091 mg/L, while the EC_{50} value of compounds without heterocyclic structure
244 (**3a-p**) ranged were 98.425-188.246 mg/L. Particularly, the activity of compounds
245 **5b-g** was generally better, and the inhibitory effect on *B. cinerea* was comparable to
246 that of the positive control compound (penthiopyrad). At a concentration of 12.50
247 mg/L, the inhibition rates of *B. cinerea* were higher than 90%. Even at 3.13 mg/L,
248 their inhibition rates were higher than 50%. Among them, compound **5b** had the best
249 antifungal effect on *B. cinerea*. Its EC_{50} value was 0.490 mg/L, which was lower than
250 the EC_{50} value of penthiopyrad (0.562 mg/L). Combined with the previous reports, we
251 speculated that this result may be due to the introduction of thiophene heterocyclic
252 structure, which changes the electron cloud density of rosin-based amide compounds
253 at the molecular level [25, 26]. These results led to the enhanced membrane permeability
254 of compounds or hydrophobic interaction with specific sites of target protein.
255 Furthermore, the absorption capacity of drug molecules and interaction by receptors
256 were improved at the physiological level [27, 28].

In addition, there was certain regularity between the structure of rosin-based amide derivatives and the inhibitory activity on *B. cinerea*. Among the compounds **3a-p**, antifungal agents with electron-withdrawing groups on the benzene ring had higher inhibitory effect on *B. cinerea* than compounds with electron-donating groups (**3k-o** > **3b-j**). Especially, the compounds with halogen structures on benzene ring had the highest activity, while as **5a-n**, compounds with aromatic ring structure had the lower activity. According to the existing literature, we speculated that rosin-based amide derivatives would have larger molecular space structure due to the introduction of aromatic ring, which may result in the weakening of penetration ability of drug molecules to membranes or tissues and the absorption and transmission of drugs in fungi [29, 30]. All of these factors can block the binding of the drugs to the receptors, and in turn affect the antifungal effect of compounds [31].

In vivo* antifungal activity against *B. cinerea. The *in vivo* antifungal activity against *B. cinerea* of compound **5b** showed good effects comparable to penthiopyrad. The *PE* values were 90.00%, 78.50%, and 62.00% at a concentration of 100, 50 and 25 mg/L, respectively. The compound **5b** possessed good protective efficacy against *B. cinerea* as shown in **Figure 1c**.

Effect of dehydroabietyl amide (5b) on mycelial morphology of *B. cinerea.* After treatment with compound **5b** at 20 mg/L, the surface of mycelia cell wall showed a certain degree of damage (**Figure 2**). The surface was rough and uneven and a few small holes appeared. This showed that rosin-based amide derivatives had a certain degree of damage to the cell wall of *B. cinerea*.

Effect of dehydroabietyl amide (5b) on cell membrane permeability of *B. cinerea.* The change of relative conductivity reflects the variation of cell membrane permeability. After treatement with the antifungal agents, the mycelial relative conductivity of *B. cinerea* increased with time, but the relative conductivity of the control did not change much at different time, indicating that compound **5b** could enhance the mycelial cell membrane permeability of *B. cinerea*. Yet, the change of relative conductivity caused by compound **5b** was much larger compared to control (**Figure 1b**). According to previous reports, the cell membrane of fungi are the key action sites of the drugs, which can destroy the synthesis of phospholipid bilayer or protein and lead to the leakage of internal electrolytes [32, 33]. Combined with the change of mycelial morphology after treatment with **5b**, it can also be inferred that compound **5b** could manifest antifungal properties by destroying cell membrane structure [34]. The above reported findings revealed that the action target site of **5b** on *B. cinerea* could be cell membrane.

Effect of dehydroabietyl amide (5b) on the respiratory metabolism of *B. cinerea.* The respiratory inhibition effect of compound **5b** and typical inhibitors on *B. cinerea* mycelia are shown in **Table 2**. Compound **5b** had a strong inhibitory effect on the respiration rate of *B.cinerea* mycelia, and the inhibition rate was 48.59% when the concentration was 25 mg/L. In addition, by comparing the superposition rate of typical respiratory inhibitors and tested agents, the main inhibition pathway of tested agents on respiratory metabolism of *B. cinerea* can be inferred. The smaller superposition rate showed that there was no synergistic effect between them, which

indicated that they had the same inhibiting pathway. The superposition rates of compound **5b** with iodoacetic acid and sodium phosphate were 44.38% and 55.63%, respectively, which indicated that compound **5b** had some inhibitory effects on EMP and HMP pathways, but the superposition rates of compound **5b** with malonic acid were relatively lower (34.69%), indicating that **5b** had more obvious inhibitory effects on TCA pathway. It has been reported that TCA pathway is related to electron transport [35, 36]. Therefore, compound **5b** may inhibit the electron transport by binding to Qo site of Cyt *bc* complex, thus inhibiting the respiratory function of *B. cinerea* and achieving the antifungal effect [37, 38].

QSAR. The quantitative structure-activity relationship of rosin-based amide derivatives (**3a-p** and **5a-n**) and antifungal activity against *B. cinerea* were studied by QSAR. The molecular descriptors of rosin-based amide derivatives were screened by heuristic regression method in CODESSSA, which revealed that they were significantly related to the antifungal activity (**Table S1**). By using these molecular descriptors as independent variables and antifungal activity as dependent variables, a series of linear QSAR models with the different number of descriptors were constructed. In order to reduce the "over-parameterization" problem and elevate the prediction ability of the model, the "breaking point" rule was used to select the best number of parameters. The best QSAR model with four descriptors was obtained through linear regression analysis (**Figure 3a**). The specific results of the model are shown in **Table 3** (R^2 = 0.9587, F = 144.94, s^2 = 0.0352). The obtained best QSAR model was validated by triple internal and “leave-one-out” test [15]. The training and

323 test results are listed in **Table S2** and the average value of training set $R_{training}^2$ was
324 0.9568 and the testing set R_{test}^2 was 0.9541. By comparing the values from the three
325 models, it could be seen that the difference between them was less than 5%. These
326 results showed that the best QSAR model had good stability and prediction ability. In
327 addition, the R_{LOO}^2 = 0.9496 (obtained from the "leave-one-out" test) was similar to
328 the above values, which also confirmed the stability of the QSAR model. The
329 antifungal activity against *B. cinerea* of 30 rosin-based amide compounds involved in
330 the constructed model was predicted. The predicted antifungal activity values and the
331 difference between the experimental and the predicted values are listed in **Table S3**.
332 **Figure 3b** shows a comparison between the experimental and predicted values of
333 rosin-based amide derivatives.

334 According to the best QSAR model, there were four descriptors, namely
335 maximum net charge (q_{max}), maximum net atomic charge for an N atom (q^N_{max}), the
336 *LUMO* and dipole moment of the molecule (*DM*), closely related to the antifungal
337 activity. These descriptors contain abundant information about the relationship
338 between rosin-based amide compounds structure and their fungicidal activity, which
339 can provide guidance for designing novel rosin derivatives. q_{max} and q^N_{max} are
340 descriptors related to the charge distribution of compounds, in which N and/or S atom
341 can act as receptors for hydrogen bonding interaction and form abundant
342 intermolecular hydrogen bonds in fungi (**Figure 3c**) [39]. At the same time, the charge
343 distribution is also closely related to the electrostatic interaction between molecules [40,
344 41]. In addition, there are conjugated systems in amide structure of rosin-based

derivatives (**3a-p** and **5a-n**). Among compounds **5a-n**, thiophene, an important sulfur-containing five-membered heterocyclic compound, has a high charge density and is more prone to π-π conjugation in fungi [25]. Therefore, the antifungal effects of rosin-based amides mainly occurred through the hydrogen bonding, conjugation and electrostatic interaction between the compounds and the receptors of target. *In vitro* antifungal activity study showed that the rosin-based compounds containing thiophene heterocycles exhibit good inhibitory activity against *B. cinerea*, which was well corroborated with the results of the model. *LUMO* is an important indicator of electronic acceptance of compounds [42]. In the process of antifungal action, thiophene ring accepts electrons and forms complexes, which is beneficial to increase the sites where derivatives can participate in hydrogen bonding interaction, thus promoting the interaction between compounds and targets and achieving the antifungal effect (**Figure 3d**) [43]. *DM*, similar to the first and second descriptor of the model, reflects the polar interaction between molecules [44]. It is also a descriptor related to the charge distribution of compounds, which can lead to changes in hydrophobicity or lipophilicity of molecules, thereby enhancing the hydrogen bonding between compounds and target sites, and thus improving the antifungal effect [45, 46].

We synthesized two series of dehydroabietyl amide derivatives from rosin and then examined their inhibitory effects on fungi *V. mali, P. capsici, B. cinerea, S. sclerotiorum* and *F. oxysporum*. *In vitro* and *in vivo* antifungal activities showed that rosin-based amide compounds containing thiophene heterocycles exhibited better inhibitory effects. In particular, compound **5b** with fluorine atom had the best

antifungal effect on *B. cinerea*, and its EC_{50} was lower compared to the positive control (penthiopyrad). Physiological and biochemical studies revealed that the primary action mechanism of **5b** on *B. cinerea* can change mycelial morphology by destroying cell wall structure, increasing cell membrane permeability and inhibiting TCA pathway in respiratory metabolism. Furthermore, QSAR and SAR studies revealed that charge distribution of rosin-based amides derivatives has a key role in the antifungal activity through the hydrogen bonding, conjugation and electrostatic interaction between the compounds and the target receptors.

SUPPORTING INFORMATION

The structural characterization data of dehydroabietyl amide derivatives (**3a-p** and **5a-n)** and values of descriptor related to dehydroabietyl amide derivatives structure and their fungicidal activity against *B. cinerea*.

NOTES

The authors declare no competing financial interest.

FUNDING

This study was supported by the National Natural Science Foundation of China (31870555) and the Fundamental Research Funds for the Central Universities (2452018031).

REFERENCES

(1) Hileman, B., Synthetic pesticides still useful, needed. *Chem. Eng. News* **2000,** *78*, 12.

(2) Rother, H. A., Pesticide labels: Protecting liability or health? – Unpacking

389 "misuse" of pesticides. *Curr. Opin. Environ. Sci. Health* **2018,** *4*, 10-15.

390 (3) Whetton, R. L.; Waine, T. W.; Mouazen, A. M., Evaluating management zone
391 maps for variable rate fungicide application and selective harvest. *Comput. Electron.*
392 *Agr.* **2018,** *153*, 202-212.

393 (4) Koehler, A. M.; Shew, H. D., Effects of fungicide applications on root-infecting
394 microorganisms and overwintering survival of perennial stevia. *Crop Prot.* **2019,** *120*,
395 13-20.

396 (5) Persaud, R.; Khan, A.; Isaac, W. A.; Ganpat, W.; Saravanakumar, D., Plant
397 extracts, bioagents and new generation fungicides in the control of rice sheath blight
398 in Guyana. *Crop Prot.* **2019,** *119*, 30-37.

399 (6) Yan, W.; Wang, X.; Li, K.; Li, T. X.; Wang, J. J.; Yao, K. C.; Cao, L. L.; Zhao,
400 S. S.; Ye, Y. H., Design, synthesis, and antifungal activity of carboxamide derivatives
401 possessing 1,2,3-triazole as potential succinate dehydrogenase inhibitors. *Pestic.*
402 *Biochem. Phys.* **2019,** *156*, 160-169.

403 (7) Lv, X. H.; Ren, Z. L.; Liu, P.; Li, B. X.; Li, Q. S.; Chu, M. J.; Cao, H. Q., Design,
404 synthesis and biological evaluation of novel nicotinamide derivatives bearing a
405 substituted pyrazole moiety as potential SDH inhibitors. *Pest Manag. Sci.* **2017,** *73*,
406 1585-1592.

407 (8) Song, X. S.; Gu, K. X.; Duan, X. X.; Xiao, X. M.; Hou, Y. P.; Duan, Y. B.;
408 Wang, J. X.; Zhou, M. G., A myosin5 dsRNA that reduces the fungicide resistance
409 and pathogenicity of *Fusarium asiaticum*. *Pestic. Biochem. Phys.* **2018,** *150*, 1-9.

410 (9) Teixeira, P. H.; Lima, R. C.; Bonicontro, B. F.; Mendes, O. L.; Soares, B. A.;

411 Carneiro, J. E. S.; Paula Júnior, T. J.; Vieira, R. F., Management of white mold in
412 common bean using partial resistance and fungicide applications. *Crop Prot.* **2019**,
413 *124*, 104867.
414 (10) Ngo, H. X.; Garneau-Tsodikova, S.; Green, K. D., A complex game of hide and
415 seek: The search for new antifungals. *Med. Chem. Comm.* **2016,** *7*, 1285-1306.
416 (11) Chen, Y.; de Bruyn Kops, C.; Kirchmair, J., Data resources for the
417 computer-guided discovery of bioactive natural products. *J. Chem. Inf. Model.* **2017,**
418 *57*, 2099-2111.
419 (12) Baker, D. D.; Chu, M.; Oza, U.; Rajgarhia, V., The value of natural products to
420 future pharmaceutical discovery. *Nat. Prod. Rep.* **2007,** *24*, 1225-1244.
421 (13) Kumar, A.; Jaitak, V., Natural products as multidrug resistance modulators in
422 cancer. *Eur. J. Med. Chem.* **2019,** *176*, 268-291.
423 (14) Neale, M., The regulation of natural products as crop-protection agents. *Pest*
424 *Manag. Sci.* **2000,** *56*, 677-680.
425 (15) Gao, Y.; Wang, Y.; Li, J.; Shang, S.; Song, Z., Improved application of natural
426 forest product terpene for discovery of potential botanical fungicide. *Ind. Crop. Prod.*
427 **2018,** *126*, 103-112.
428 (16) Wang, H.; Liu, B.; Liu, X.; Zhang, J.; Xian, M., Synthesis of biobased epoxy
429 and curing agents using rosin and the study of cure reactions. *Green Chem.* **2008,** *10*,
430 1190-1196.
431 (17) Yu, J.; Liu, Y.; Liu, X.; Wang, C.; Wang, J.; Chu, F.; Tang, C., Integration of
432 renewable cellulose and rosin towards sustainable copolymers by “grafting from”

433 ATRP. *Green Chem.* **2014,** *16*, 1854-1864.

434 (18) Wei, W.; Cheng, D.; Liu, J.; Li, Y.; Ma, Y.; Li, Y.; Yu, S.; Zhang, X.; Li, Z.,
435 Design, synthesis and SAR study of novel sulfonylureas containing an alkenyl
436 moiety. *Org. Biomol. Chem.* **2016,** *14*, 8356-8366.

437 (19) Xing, Y.; Xu, Q.; Che, Z.; Li, X.; Li, W., Effects of chitosan-oil coating on blue
438 mold disease and quality attributes of jujube fruits. *Food Funct.* **2011,** *2*, 466-474.

439 (20) Saravia, L. P. H.; Anandhakumar, S.; Parussulo, A. L. A.; Matias, T. A.;
440 Caldeira da Silva, C. C.; Kowaltowski, A. J.; Araki, K.; Bertotti, M., Development of
441 a tetraphenylporphyrin cobalt (II) modified glassy carbon electrode to monitor oxygen
442 consumption in biological samples. *J. Electroanal. Chem.* **2016,** *775*, 72-76.

443 (21) Koyambo-Konzapa, S. J.; Dhaouadi, Z.; Nsangou, M., Hydration of
444 l-glycylvaline and l-glycylvalylglycine zwitterions: Structural and vibrational studies
445 using DFT method. *J. Mol. Graph. Model.* **2019,** *88*, 194-202.

446 (22) Li, J.; Lin, H. X.; Chen, X. Y.; Zhu, J. R.; Yang, M. S.; Yang, J.; Han, C. R.,
447 Self-assembled structures and excellent surface properties of a novel anionic
448 phosphate diester surfactant derived from natural rosin acids. *J. Colloid Interf. Sci.*
449 **2017,** *486*, 67-74.

450 (23) Wilbon, P. A.; Chu, F.; Tang, C., Progress in renewable polymers from natural
451 terpenes, terpenoids, and rosin. *Macromol. Rapid Comm.* **2013,** *34*, 8-37.

452 (24) Cabaret, T.; Gardere, Y.; Frances, M.; Leroyer, L.; Charrier, B., Measuring
453 interactions between rosin and turpentine during the drying process for a better
454 understanding of exudation in maritime pine wood used as outdoor siding. *Ind. Crop.*

Prod. **2019,** *130*, 325-331.

(25) Karcı, F.; Karcı, F., Synthesis and tautomeric structures of some novel thiophene-based bis-heterocyclic monoazo dyes. *J. Mol. Struct.* **2012,** *1024*, 117-122.

(26) Borisov, D. D.; Chermashentsev, G. R.; Novikov, R. A.; Tomilov, Y. V., "Four-component" assembly of polyaromatic 4H-cyclopenta[b]thiophene structures based on $GaCl_3$-promoted reaction of styrylmalonates with 5-phenylthiophene-2-carbaldehyde. *Tetrahedron Lett.* **2019,** *60*, 746-750.

(27) Mugnaini, C.; Rabbito, A.; Brizzi, A.; Palombi, N.; Petrosino, S.; Verde, R.; Di Marzo, V.; Ligresti, A.; Corelli, F., Synthesis of novel 2-(1-adamantanylcarboxamido)thiophene derivatives. Selective cannabinoid type 2 (CB2) receptor agonists as potential agents for the treatment of skin inflammatory disease. *Eur. J. Med. Chem.* **2019,** *161*, 239-251.

(28) Berryman, O. B.; Johnson, C. A.; Vonnegut, C. L.; Fajardo, K. A.; Zakharov, L. N.; Johnson, D. W.; Haley, M. M., Solid-state examination of conformationally diverse sulfonamide receptors based on bis (2-anilinoethynyl)pyridine, -bipyridine, and -thiophene. *Cryst. Growth Des.* **2015,** *15*, 1502-1511.

(29) Gómez, E. C.; Anguiano Igea, S.; Gómez Amoza, J. L.; Otero Espinar, F. J., Evaluation of the promoting effect of soluble cyclodextrins in drug nail penetration. *Eur. J. Pharm. Sci.* **2018,** *117*, 270-278.

(30) Zhuang, C.; Guan, X.; Ma, H.; Cong, H.; Zhang, W.; Miao, Z., Small molecule-drug conjugates: A novel strategy for cancer-targeted treatment. *Eur. J. Med. Chem.* **2019,** *163*, 883-895.

(31) Noorizadeh, H.; Sobhan Ardakani, S.; Ahmadi, T.; Mortazavi, S. S.; Noorizadeh, M., Application of genetic algorithm-kernel partial least square as a novel non-linear feature selection method: partitioning of drug molecules. *Drug Test. Anal.* **2013,** *5*, 89-95.

(32) Ma, Y. N.; Xu, F. R.; Chen, C. J.; Li, Q. Q.; Wang, M. Z.; Cheng, Y. X.; Dong, X., The beneficial use of essential oils from buds and fruit of Syzygium aromaticum to combat pathogenic fungi of Panax notoginseng. *Ind. Crop. Prod.* **2019,** *133*, 185-192.

(33) Xu, L.; Tao, N.; Yang, W.; Jing, G., Cinnamaldehyde damaged the cell membrane of Alternaria alternata and induced the degradation of mycotoxins *in vivo*. *Ind. Crop. Prod.* **2018,** *112*, 427-433.

(34) Asamov, D. K.; Tursunkulova, R. K.; Isaev, P. I.; Otroshchenko, O. S.; Stepanichenko, N. N., The action of phytotoxic substances of the fungusVerticillium dahliae on the permeability of a synthetic phospholipid membrane. *Chem. Nat. Compd.* **1975,** *11*, 713-714.

(35) Alonso-Garrido, M.; Escrivá, L.; Manyes, L.; Font, G., Enniatin B induces expression changes in the electron transport chain pathway related genes in lymphoblastic T-cell line. *Food. Chem. Toxicol.* **2018,** *121*, 437-443.

(36) McDonald, A. E.; Pichaud, N.; Darveau, C. A., "Alternative" fuels contributing to mitochondrial electron transport: Importance of non-classical pathways in the diversity of animal metabolism. *Comp. Biochem. Phys. B* **2018,** *224*, 185-194.

(37) Schäff, C.; Börner, S.; Hacke, S.; Kautzsch, U.; Albrecht, D.; Hammon, H. M.;

499 Röntgen, M.; Kuhla, B., Increased anaplerosis, TCA cycling, and oxidative
500 phosphorylation in the liver of dairy cows with intensive body fat mobilization during
501 early lactation. *J. Proteome Res.* **2012,** *11*, 5503-5514.
502 (38) Li, L.; Kitazawa, H.; Wang, X.; Sun, H., Regulation of respiratory pathway and
503 electron transport chain in relation to senescence of postharvest white mushroom
504 (*Agaricus bisporus*) under high O_2/CO_2 controlled atmospheres. *J. Agr. Food Chem.*
505 **2017,** *65*, 3351-3359.
506 (39) Collins, K. D., Charge density-dependent strength of hydration and biological
507 structure. *Biophys. J.* **1997,** *72*, 65-76.
508 (40) Bojarowski, S. A.; Kumar, P.; Wandtke, C. M.; Dittrich, B.; Dominiak, P. M.,
509 Universal method for electrostatic interaction energies estimation with charge
510 penetration and easily attainable point charges. *J. Chem. Theory Comput.* **2018,** *14*,
511 6336-6345.
512 (41) van der Lubbe, S. C. C.; Zaccaria, F.; Sun, X.; Fonseca Guerra, C., Secondary
513 electrostatic interaction model revised: Prediction comes mainly from measuring
514 charge accumulation in hydrogen-bonded monomers. *J. Am. Chem. Soc.* **2019,** *141*,
515 4878-4885.
516 (42) Barim, E.; Akman, F., Synthesis, characterization and spectroscopic
517 investigation of N-(2-acetylbenzofuran-3-yl)acrylamide monomer: Molecular
518 structure, HOMO–LUMO study, TD-DFT and MEP analysis. *J. Mol. Struct.* **2019,**
519 *1195*, 506-513.
520 (43) Tighadouini, S.; Radi, S.; Abrigach, F.; Benabbes, R.; Eddike, D.; Tillard, M.,

Novel *β*-keto–enol pyrazolic compounds as potent antifungal agents. Design, synthesis, crystal structure, DFT, homology modeling, and docking studies. *J. Chem. Inf. Model*. **2019,** *59*, 1398-1409.

(44) Saiz-Urra, L.; Racero, J. C.; Macías-Sánchez, A. J.; Hernández-Galán, R.; Hanson, J. R.; Perez-Gonzalez, M.; Collado, I. G., Synthesis and quantitative structure−antifungal activity relationships of clovane derivatives against *Botrytis cinerea*. *J. Agr. Food Chem.* **2009,** *57*, 2420-2428.

(45) Gao, Y. M.; Wang, X. J.; Zhang, J.; Li, M.; Liu, C. X.; An, J.; Jiang, L.; Xiang, W. S., Borrelidin, A potent antifungal agent: Insight into the antifungal mechanism against *Phytophthora sojae*. *J. Agr. Food Chem.* **2012,** *60*, 9874-9881.

(46) Mohapatra, R. K.; Sarangi, A. K.; Azam, M.; El-ajaily, M. M.; Kudrat-E-Zahan, M.; Patjoshi, S. B.; Dash, D. C., Synthesis, structural investigations, DFT, molecular docking and antifungal studies of transition metal complexes with benzothiazole based Schiff base ligands. *J. Mol. Struct.* **2019,** *1179*, 65-75.

535 **FIGURE CAPTIONS**

536 **Scheme 1**. Synthesis route of rosin-based amide (**3a-p**)

537 **Scheme 2**. Synthesis route of rosin-based amide with thiophene heterocyclic structure

538 (**5a-n**)

539 **Figure 1.** (a) *In vitro* antifungal effects of compound **5b** on *B. cinerea*; (b) Mycelial

540 relative conductivity of *B. cinerea* in the presence or absence of **5b**; (c) The protective

541 efficacy of compound **5b** and penthiopyrad (at a concentration of 100, 50 and 25

542 mg/L, respectively) on strawberry leaves inoculated with *B. cinerea* by *in vivo* tissue

543 method

544 **Figure 2.** Effect of compound **5b** on mycelial morphology in *B. cinerea*. (a, b): 1.00K

545 times, plates untreated and treated with the concentration of EC_{50} values of **5b**; (c, d):

546 3.00K times, plates untreated and treated with the concentration of EC_{50} values of **5b**

547 **Figure 3.** (a) The "breaking point" rule was used to confirm the number of descriptors

548 of the QSAR model. (b) The experimental and predicted values of antifungal activity

549 against *B. cinerea* of rosin-based amide derivatives using the built QSAR model. (c)

550 The charge distribution, MEP plot and contour map of compound **5b** from DFT

551 calculation of Gaussian 16W. (d) *LUMO* energy map of compound **5b**

552 **Table 1 Antifungal activities of rosin-based derivatives (3a-p and 5a-n) against *B. cinerea***

compound	*IR* (%) at a concentration of (mg/L) ± standard deviation (SD; n ≥ 3)										EC_{50}	*y*=a+b*x*	R^2	log EC_{50}
	500.00	200.00	100.00	50.00	25.00	12.50	6.25	3.13	1.56	0.78				
3a	100.00 ± 0.00 a	80.00 ± 1.00 b	40.00 ± 0.90 c	22.00 ± 0.50 e	12.50 ± 0.05 e	5.60 ± 0.03 f	/	/	/	/	125.944	*y*=-2.751+0.022*x*	0.963	2.100
3b	100.00 ± 0.00 a	73.00 ± 1.14 b	38.00 ± 0.93 c	19.50 ± 0.61e	11.90 ± 0.08 e	5.50 ± 0.07 f	/	/	/	/	138.152	*y*=-2.746+0.020*x*	0.956	2.140
3c	100.00 ± 0.00 a	75.00 ± 0.80 b	39.40 ± 0.99 c	20.00 ± 0.55 e	12.50 ± 0.06 e	6.00 ± 0.03 f	/	/	/	/	133.897	*y*=-2.713+0.020*x*	0.963	2.127
3d	100.00 ± 0.00 a	76.00 ± 0.92 b	39.80 ± 1.00 c	20.00 ± 0.62 e	12.80 ± 0.05 e	5.99 ± 0.02 f	/	/	/	/	132.159	*y*=-2.715+0.021*x*	0.964	2.121
3e	100.00 ± 0.00 a	75.00 ± 0.94 b	39.50 ± 1.10 c	20.10 ± 0.43 e	12.60 ± 0.03 e	6.00 ± 0.08 f	/	/	/	/	133.754	*y*=-2.707+0.020*x*	0.962	2.126
3f	100.00 ± 0.00 a	69.00 ± 0.95 b	34.00 ± 0.92 d	15.20 ± 0.24 e	9.50 ± 0.02 f	3.89 ± 0.05 f	/	/	/	/	149.358	*y*=-2.989+0.020*x*	0.948	2.174
3g	100.00 ± 0.00 a	70.00 ± 0.88 b	34.00 ± 0.95 d	15.00 ± 0.08 e	9.50 ± 0.04 f	4.00 ± 0.02 f	/	/	/	/	148.001	*y*=-3.003+0.020*x*	0.955	2.170
3h	98.00 ± 1.92 a	54.00 ± 0.98 c	28.00 ± 0.98 d	12.20 ± 0.15 e	6.50 ± 0.01 f	/	/	/	/	/	187.390	*y*=-3.129+0.017*x*	0.989	2.273
3i	98.00 ± 1.31 a	54.00 ± 0.69 c	27.00 ± 1.03 d	12.00 ± 0.18 e	6.30 ± 0.03 f	/	/	/	/	/	188.246	*y*=-3.164+0.017*x*	0.989	2.275
3j	98.00 ± 2.10 a	54.00 ± 0.85 c	27.50 ± 0.80 d	12.10 ± 0.07 e	6.50 ± 0.02 f	/	/	/	/	/	187.813	*y*=-3.142+0.017*x*	0.990	2.274
3k	100.00 ± 0.00 a	94.00 ± 0.91 a	42.30 ± 1.41 c	30.25 ± 0.39 d	16.15 ± 0.25 e	9.20 ± 0.09 f	5.07 ± 0.03 f	/	/	/	100.061	*y*=-2.491+0.025*x*	0.968	2.000
3l	100.00 ± 0.00 a	94.00 ± 1.29 a	42.30 ± 1.20 c	30.25 ± 0.25 d	16.30 ± 0.54 e	9.00 ± 0.14 f	4.99 ± 0.04 f	/	/	/	100.074	*y*=-2.495+0.025*x*	0.967	2.000
3m	100.00 ± 0.00 a	90.00 ± 1.10 a	42.00 ± 0.90 c	28.00 ± 0.40 d	15.30 ± 0.17 e	9.60 ± 0.13 f	5.00 ± 0.06 f	/	/	/	106.456	*y*=-2.453+0.023*x*	0.967	2.027
3n	100.00 ± 0.00 a	95.00 ± 1.48 a	43.00 ± 0.75 c	30.00 ± 0.25 d	16.30 ± 0.30 e	9.00 ± 0.18 f	4.99 ± 0.02 f	/	/	/	98.425	*y*=-2.524+0.026*x*	0.970	1.993
3o	100.00 ± 0.00 a	88.00 ± 0.92 b	42.00 ± 0.92 c	28.00 ± 0.50 d	15.30 ± 0.28 e	9.60 ± 0.12 f	5.00 ± 0.03 f	/	/	/	109.005	*y*=-2.414+0.022*x*	0.962	2.037
3p	100.00 ± 0.00 a	83.00 ± 1.83 b	40.00 ± 1.00 c	25.00 ± 0.80 d	14.00 ± 0.09 e	8.60 ± 0.17 f	/	/	/	/	119.679	*y*=-2.603+0.022*x*	0.985	2.078
5a	100.00 ± 0.00 a	100.00 ± 0.00 a	100.00 ± 0.00 a	100.00 ± 0.00 a	98.00 ± 2.50 a	89.00 ± 1.95 a	65.00 ± 1.02 b	40.00 ± 1.12 b	26.00 ± 0.90 b	/	5.614	*y*=-1.952+0.348*x*	0.964	0.749
5b	100.00 ± 0.00 a	100.00 ± 0.00 a	100.00 ± 0.00 a	100.00 ± 0.00 a	100.00 ± 0.00 a	99.44 ± 2.21 a	92.78 ± 1.91 a	75.30 ± 1.20 a	61.46 ± 1.02 a	53.48 ± 1.04 a	0.490	*y*=-0.213+0.435*x*	0.999	-0.310
5c	100.00 ± 0.00 a	100.00 ± 0.00 a	100.00 ± 0.00 a	100.00 ± 0.00 a	100.00 ± 0.00 a	99.10 ± 1.93 a	91.60 ± 2.00 a	73.21 ± 0.95 a	59.78 ± 0.85 a	51.03 ± 1.12 a	0.652	*y*=-0.271+0.416*x*	0.998	-0.186
5d	100.00 ± 0.00 a	100.00 ± 0.00 a	100.00 ± 0.00 a	100.00 ± 0.00 a	100.00 ± 0.00 a	98.67 ± 2.90 a	90.12 ± 1.86 a	72.02 ± 1.42 a	58.14 ± 1.10 a	46.22 ± 1.20 a	0.917	*y*=-0.374+0.408*x*	0.997	-0.038
5e	100.00 ± 0.00 a	100.00 ± 0.00 a	100.00 ± 0.00 a	100.00 ± 0.00 a	100.00 ± 0.00 a	99.03 ± 2.21 a	90.70 ± 1.50 a	72.31 ± 1.90 a	59.28 ± 1.23 a	47.03 ± 0.95 a	0.865	*y*=-0.364+0.421*x*	0.998	-0.063
5f	100.00 ± 0.00 a	100.00 ± 0.00 a	100.00 ± 0.00 a	100.00 ± 0.00 a	100.00 ± 0.00 a	96.10 ± 2.00 a	88.12 ± 1.38 a	70.32 ± 1.66 a	50.30 ± 0.90 a	41.28 ± 0.90 b	1.343	*y*=-0.484+0.360*x*	0.958	0.128
5g	100.00 ± 0.00 a	100.00 ± 0.00 a	100.00 ± 0.00 a	100.00 ± 0.00 a	100.00 ± 0.00 a	93.00 ± 1.80 a	82.52 ± 1.57 b	51.08 ± 1.24 b	42.30 ± 1.00 b	36.58 ± 0.76 b	2.526	*y*=-0.778+0.308*x*	0.956	0.402
5h	100.00 ± 0.00 a	100.00 ± 0.00 a	90.00 ± 2.20 a	65.00 ± 1.10 b	67.88 ± 1.00 b	41.60 ± 0.90 c	35.50 ± 1.04 d	22.00 ± 0.60 d	/	/	40.443	*y*=-2.181+0.054*x*	0.984	1.607
5i	100.00 ± 0.00 a	100.00 ± 0.00 a	80.00 ± 2.10 b	48.55 ± 0.96 c	27.15 ± 0.56 d	18.20 ± 0.20 e	9.30 ± 0.20 f	/	/	/	50.498	*y*=-2.320+0.046*x*	0.966	1.703
5j	100.00 ± 0.00 a	100.00 ± 0.00 a	100.00 ± 0.00 a	96.00 ± 2.00 a	67.00 ± 1.12 b	50.18 ± 1.51 c	40.40 ± 0.95 c	31.81 ± 0.97 c	24.80 ± 0.80 b	/	14.986	*y*=-1.420+0.095*x*	0.987	1.176
5k	100.00 ± 0.00 a	100.00 ± 0.00 a	100.00 ± 0.00 a	97.00 ± 0.98 a	67.00 ± 0.90 b	50.50 ± 1.20 c	40.40 ± 1.20 c	31.25 ± 1.24 c	25.00 ± 0.76 b	/	14.770	*y*=-1.448+0.098*x*	0.984	1.169
5l	100.00 ± 0.00 a	100.00 ± 0.00 a	100.00 ± 0.00 a	81.20 ± 1.50 b	52.40 ± 0.82 c	25.90 ± 0.35 e	21.00 ± 0.80 e	11.00 ± 0.06 d	/	/	27.794	*y*=-2.484+0.089*x*	0.967	1.444
5m	100.00 ± 0.00 a	100.00 ± 0.00 a	100.00 ± 0.00 a	82.30 ± 1.38 b	51.80 ± 1.13 c	24.90 ± 0.40 e	22.00 ± 0.72 e	10.80 ± 0.05 d	/	/	27.597	*y*=-2.503+0.091*x*	0.967	1.441
5n	100.00 ± 0.00 a	100.00 ± 0.00 a	64.00 ± 1.23 b	32.55 ± 0.25 d	16.15 ± 0.33 e	9.20 ± 0.09 f	4.67 ± 0.03 f	/	/	/	78.091	*y*=-3.277+0.042*x*	0.951	1.893
penthiopyrad	100.00 ± 0.00 a	100.00 ± 0.00 a	100.00 ± 0.00 a	100.00 ± 0.00 a	100.00 ± 0.00 a	99.30 ± 2.90 a	91.80 ± 2.21 a	74.60 ± 1.08 a	60.46 ± 1.02 a	52.23 ± 1.20 a	0.562	*y*=-0.237+0.422*x*	0.999	

553 Values in columns followed by similar letters were not significantly different according to Fisher's protected LSD test ($P < 0.05$)

554 **Table 2 The respiratory inhibition rate and superposition rate of compound 5b**

555 **and typical inhibitors on *B. cinerea* mycelia**

inhibitors	R_0 (O_2, μmol/g·min)	R_1 (R_1') (O_2, μmol/g·min)	IR_r (%)	R_R (%)
malonic acid	12.45 ± 0.30 a	8.30 ± 0.06 a	33.33	/
iodoacetic acid	12.45 ± 0.28 a	7.85 ± 0.03 a	36.95	/
sodium phosphate	12.45 ± 0.26 a	7.05 ± 0.04 b	43.37	/
5b	12.45 ± 0.29 a	6.40 ± 0.06 c	48.59	/
5b and malonic acid	12.45 ± 0.27 a	4.18 ± 0.03 d	66.43	34.69
5b and iodoacetic acid	12.45 ± 0.28 a	3.56 ± 0.04 e	71.41	44.38
5b and sodium phosphate	12.45 ± 0.29 a	2.84 ± 0.03 f	77.19	55.63

556 R_0, R_1 and R_1'are respiration rate of mycelia before adding tested agents, after adding tested agents

557 and after adding tested agents with typical inhibitors; IR_r is the inhibition rate of mycelia

558 respiration; R_R is the superposition rate of tested agents with typical inhibitors. All results are

559 presented as the mean ± standard deviation (SD; n ≥ 3).

560 **Table 3 The constructed model with four optimum descriptors**

descriptor No.	X	$\pm \Delta X$	t-test	descriptor
0	1.2767e+01	3.2808e+00	3.8914	Intercept
1	3.3232e-01	6.4745e-02	5.1327	q_{max} [a]
2	-3.9091e+00	2.5005e-01	-15.6331	q^{N}_{max} [b]
3	8.2097e-02	7.3287e-03	11.2021	$LUMO$ [c]
4	-8.1504e+00	1.7601e+00	-4.6306	DM [d]

561 [a] Maximum net charge. [b] Maximum net atomic charge for an N atom. [c] The lowest unoccupied

562 molecular orbital. [d] Dipole moment of the molecule.

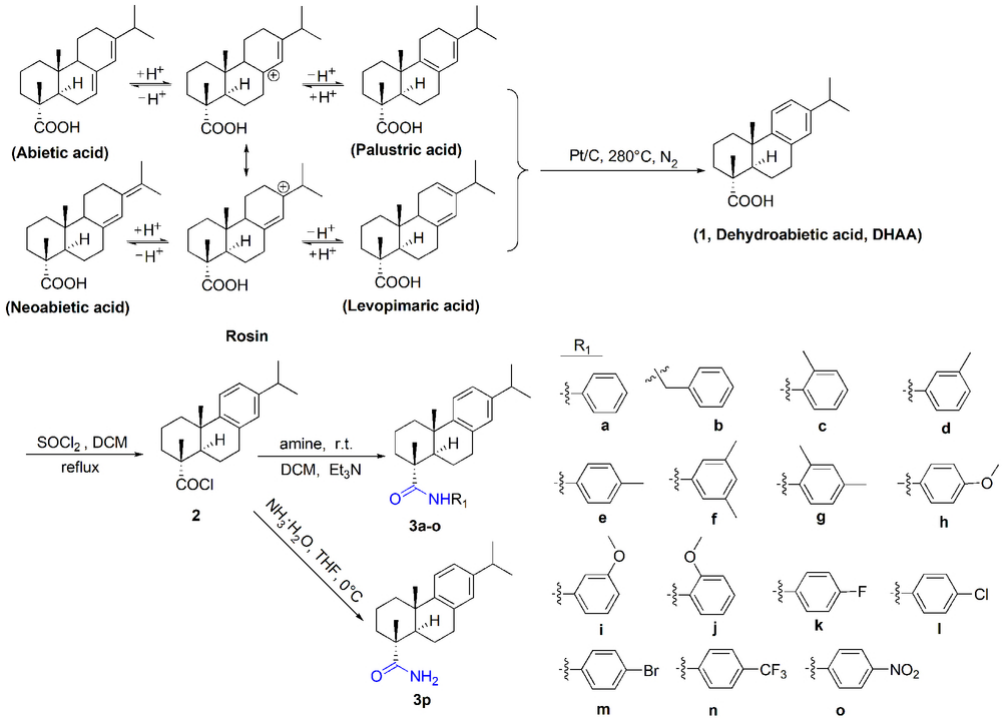

Scheme 1

84x60mm (300 x 300 DPI)

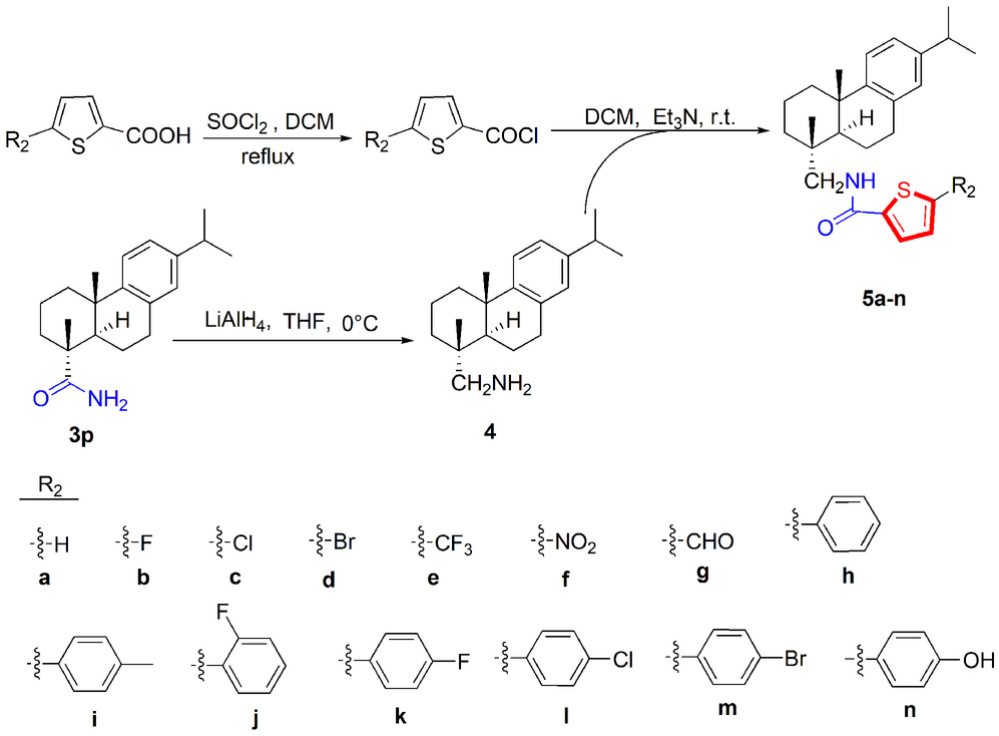

Scheme 2

84x61mm (300 x 300 DPI)

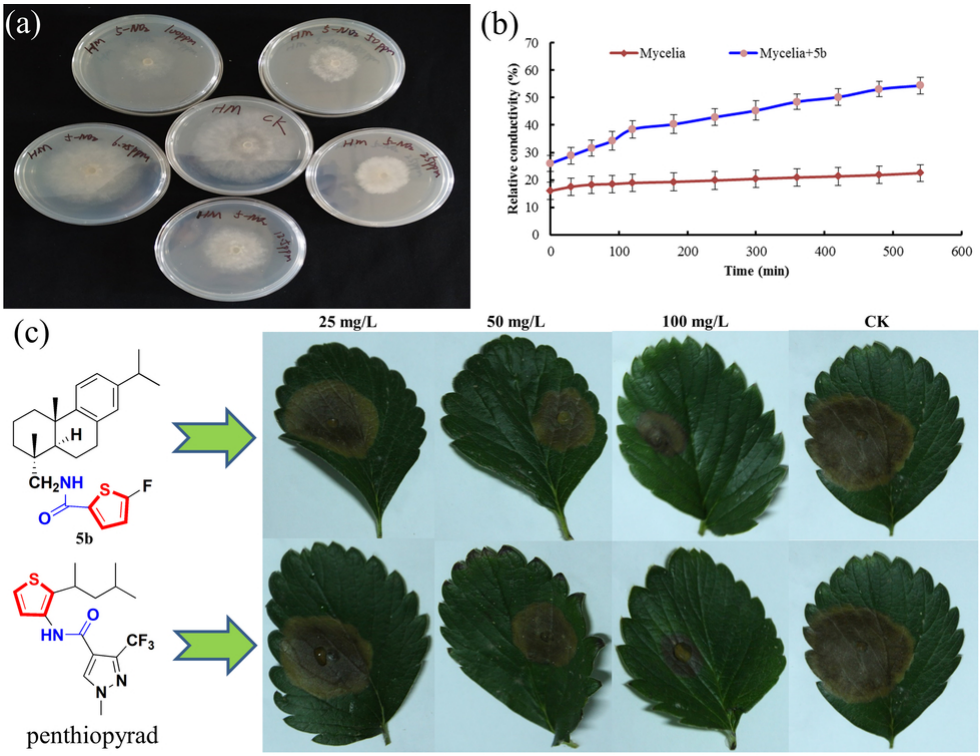

Figure 1

84x63mm (300 x 300 DPI)

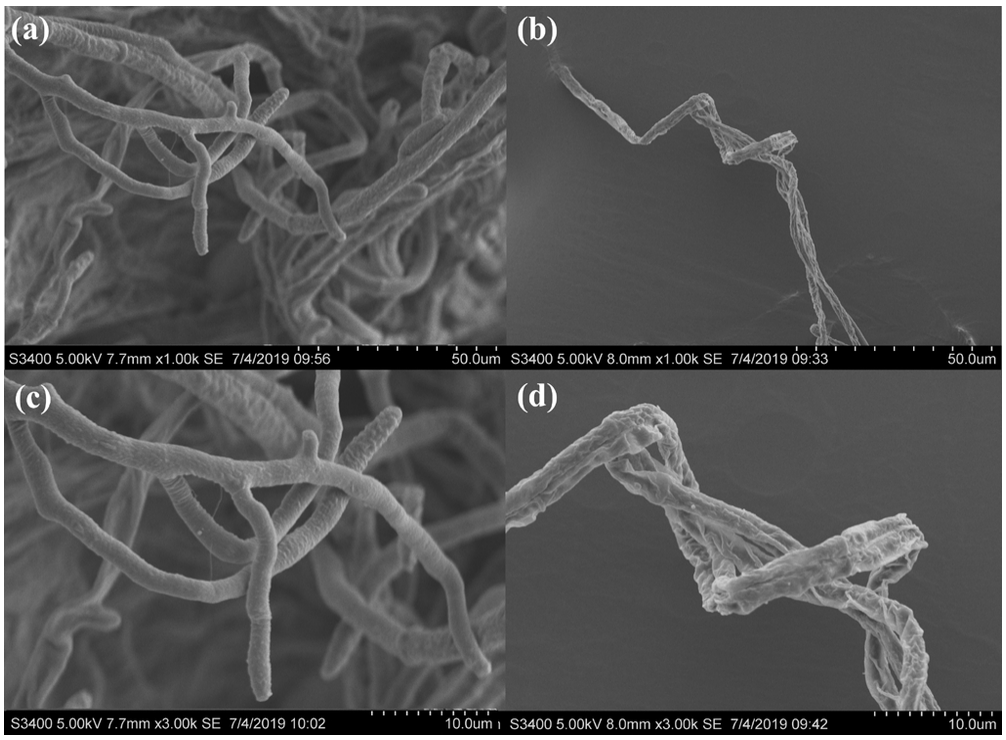

Figure 2

84x61mm (300 x 300 DPI)

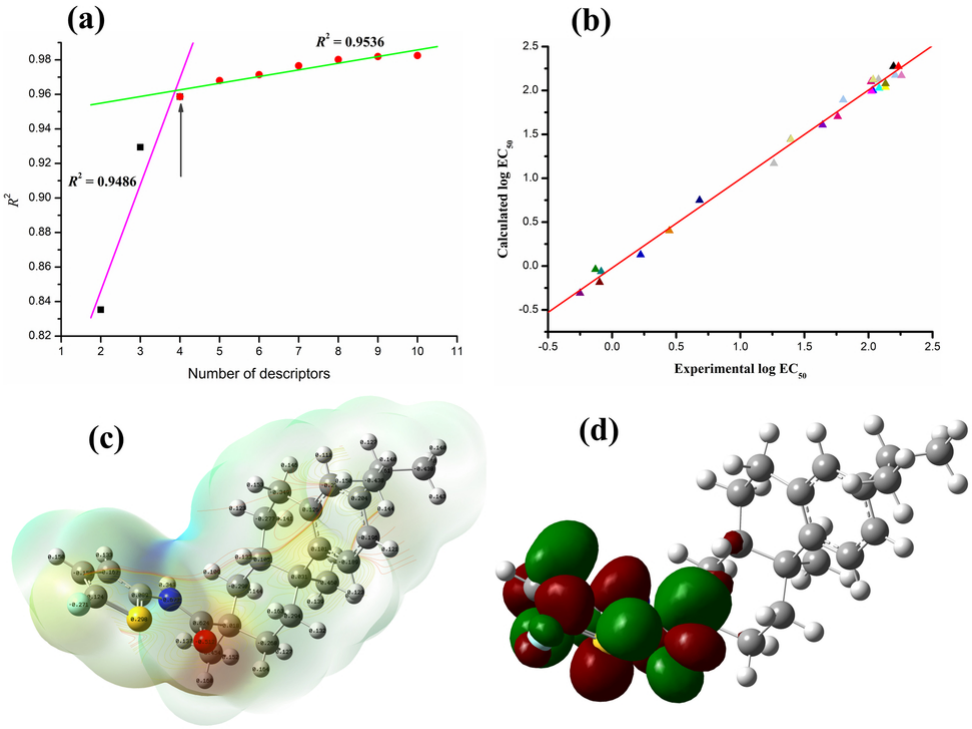

Figure 3

84x63mm (300 x 300 DPI)

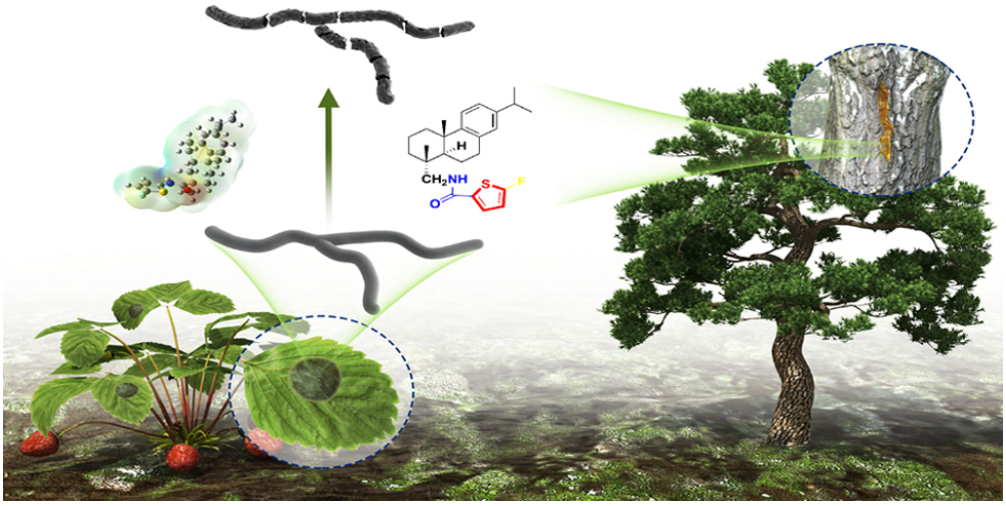

Graphic for table of contents

82x44mm (300 x 300 DPI)